https://doi.org/10.5194/amt-2021-234
Preprint. Discussion started: 10 August 2021

Atmospheric Measurement Techniques Discussions

The Antarctic Stratospheric Aerosol Observation and Sample-Return System Using Two-Stage Separation Method of a Balloon-Assisted Unmanned Aerial Vehicle

Shin-Ichiro Higashino[1], Masahiko Hayashi[2], Takuya Okada[3], Shuji Nagasaki[1], Koichi Shiraishi[2], Keiichi Ozuka[4]

[1]Department of Aeronautics and Astronautics, Kyushu University, Fukuoka, 819-0395, Japan
[2]Department of Earth System Science, Fukuoka, 814-0180, Japan
[3]Graduate Student, Kyushu University, Fukuoka, 819-0395, Japan
[4]Nippon Tungsten Co.,Ltd., Saga, 841-0203, Japan

Correspondence to: Shin-Ichiro Higashino (tonton@aero.kyushu-u.ac.jp)

Abstract The authors have developed a system for the Antarctic stratospheric aerosol observation and sample-return using the combination of a rubber balloon, a parachute, and a gliding fixed-wing unmanned aerial vehicle (UAV). A rubber balloon can usually reach 20km to 30km in altitude, but it becomes difficult for the UAV designed as a low-subsonic UAV to directly glide back from the stratospheric altitudes because the quantitative aerodynamic characteristics necessary for the control system design at such altitudes are difficult to obtain. In order to make the observation and sample-return possible at such higher altitudes while avoiding the problem with the control system of the UAV, the method using the two-stage separation was developed and attempted in Antarctica. In two-stage separation method, the UAV first descends by a parachute after separating from the balloon at stratospheric altitude to a certain altitude wherein the flight control system of the UAV works properly. Then it secondly separates the parachute for autonomous gliding back to the released point on the ground. The UAV in which an optical particle counter and an airborne aerosol sampler were installed was launched on January 24, 2015 from S17 (69.028S, 40.093E, 607 m MSL) near Syowa Station in Antarctica. The system reached 23km in altitude and the UAV successfully returned aerosol samples. In this paper, the details of the UAV system using the two-stage separation method including the observation flight results, and the preliminary results of the observation and analyses of the samples are shown.

1 Introduction

Various aerosols are drifting in the atmosphere and have influences on weather and climate change through the global heat balance and material balance (Stocker et al., 2013). Most of Antarctic surface is covered by thick ice for all year around, and Antarctica is the furthest place from the places where activities of live animals and plants, and artificial economic activities are conducted. Thus Antarctica is an optimal place for the observation of background aerosol because the concentration of aerosol is about a few percent of that in other areas. Antarctica is one of the cold sources in the global heat balance, but its

https://doi.org/10.5194/amt-2021-234
Preprint. Discussion started: 10 August 2021


Atmospheric Measurement Techniques Discussions

direct effect through aerosol is not so large because the amount of aerosol is small. However, it has something to do with the heat balance indirectly through clouds and precipitation, and the understanding of the distribution and varying mechanisms of them is indispensable not only for understanding the material balance and climate change prediction.

Various aerosol observations have been conducted in the past, and several insights regarding the feature of the distribution and changing mechanisms of aerosols were obtained (Yamanouchi, 2010). However, the observation in Antarctica is forced to be conducted under various constraints such as low temperature, long polar nights, and insufficient observation facilities. There are several methods for the observation of aerosol concentration and aerosol sampling such as the method using a rubber balloon (Ito et al., 1986, Hayashi et.al., 1998, Hara et al., 2014), a tethered balloon (Hara et al., 2013), and a manned airplane (Iwasaka et al., 1985, Yamanouchi et al., 1999, Hara et al., 2006). All methods have advantages and disadvantages in terms of reachable altitude, cost, easiness of sample retrieval, required labour, and so on. The maximum observation altitude using a rubber balloon typically reaches about 20 to 30km which is far beyond that of a tethered balloon and a manned airplane, while its operation is relatively handy and its cost is low. However, it is often difficult especially in Antarctica to retrieve the observation instruments and aerosol samples which fell down on the surface of the ice floor or the frozen sea after the burst of the balloon. It is a big problem that we have almost no choice but to discard the expensive observation apparatuses which cost approximately ten thousand US$/unit every time. It is even fatal that we cannot retrieve the precious aerosol samples. Such problems hardly occur for a tethered balloon, but the reachable altitude is limited up to only several kilometres due to the strength and weight of a tether line. There are also no such limitations for manned airplanes, but the maximum reachable altitude is at most the lower layer of the stratosphere which is far below that of a free balloon. The operating cost of a manned airplane is huge compared to that of the method using a free balloon and a tethered balloon, and the cumbersome arrangement of flight schedule is always required unless we possess our own airplane and operating staffs. In particular, in order to operate manned airplanes in Antarctica, it requires not only huge cost but also requires several additional operational loads including the maintenance of the runway.

Unmanned Aerial Vehicles (UAVs) have made a rapid progress after the 21st century due to the progress of several technologies such as microcomputers, micro electro mechanical system (MEMS) sensors, and the GPS navigation system. The UAVs are indispensable for military operations these days, and the number of scientific operations is also increasing in Polar region wherein the operation of manned airplanes is difficult. (Spiess et al.,2007, BAS,2008, Higashino et al.,2013, Higashino et al., 2014, Funaki et al.,2014). The authors have developed an innovative aerosol observation and sample-return system using the combination of a free balloon and a UAV (Higashino et al.,2014, Higashino et al, 2020). The system has proved its high capability by the five observation flights in Antarctica as one of the summer activities of the 54th Japanese Antarctic Research Expedition (JARE54) in 2014 in which the aerosol samples were retrieved successfully from the maximum altitude of 10km by the gliding UAV. This aerosol observation and sample-return method enabled not only the retrieval of the expensive observation instruments such as an optical particle counter (OPC) and an airborne aerosol sampler (AAS), but also enabled the retrieval of the priceless aerosol samples which are sometimes difficult to retrieve in the method using just a free balloon. On the other hand, the maximum altitude where aerosol samples were collected was 10km in 2014, and it is not high enough

https://doi.org/10.5194/amt-2021-234
Preprint. Discussion started: 10 August 2021

compared to the typical reachable altitude of a rubber balloon. However, it is not easy to raise the start altitude of the UAV for gliding. It is mainly because the air density and pressure at higher altitudes decreases rapidly as the altitude increases in stratosphere, and the air density at 30km becomes approximately 1/100 of that at sea level. It causes various problems for the UAV, and it is difficult to design the control system of the UAV without knowing the aerodynamic characteristics at such higher altitudes. In order to avoid this problem, the authors have devised the method named "two-stage separation method".

2 Aerosol observation and sample-return method using two-stage separation

How the method for aerosol observation and sample-return using the two-stage separation method works is shown in Fig.1. The observation and sampling instruments are installed in the UAV, and the UAV climbs up using the buoyancy of a balloon while observation and sampling are performed during the climb (Fig.1, 1). After reaching the maximum altitude, the balloon bursts or the UAV firstly separates the balloon intentionally and automatically (Fig.1, 2). The UAV descends down using a parachute to an altitude wherein the flight control system of the UAV works properly (Fig.1, 3). Then the UAV secondly separates the parachute automatically (Fig.1, 4), and starts gliding back to the sky over the released point on the ground autonomously (Fig.1, 5). The UAV descends down along the spiral glide path over the released point on the ground, and is recovered by a recovery parachute. (Fig.1, 6) This method enabled not only the aerosol observation and sampling up to high

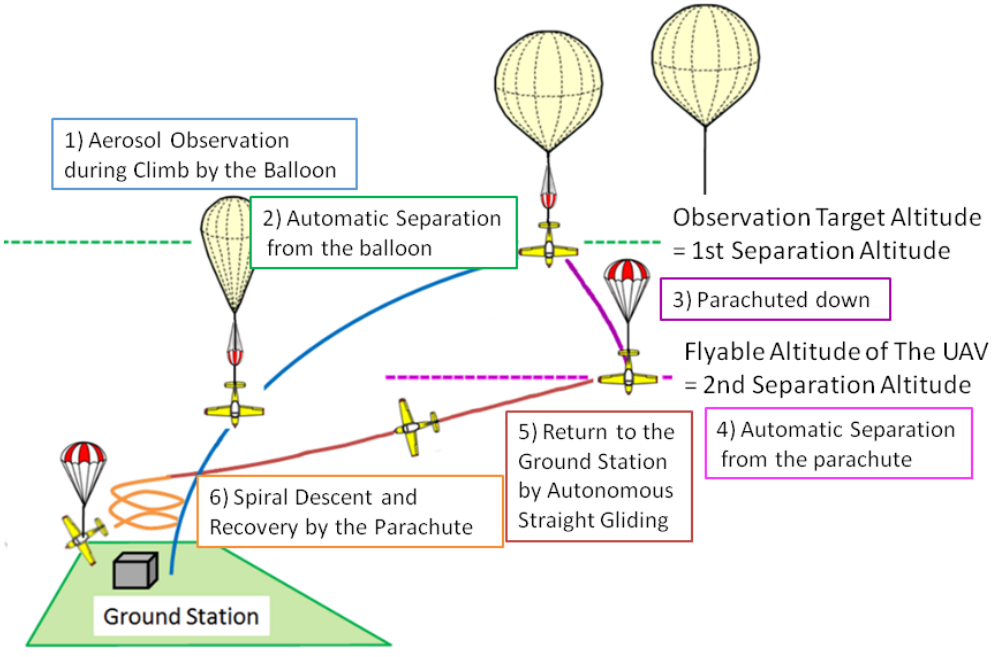

Fig.1 Aerosol observation and sample-return using the two-stage separation method

https://doi.org/10.5194/amt-2021-234
Preprint. Discussion started: 10 August 2021

Atmospheric Measurement Techniques Discussions

stratospheric altitude, but also the retrieval of the expensive aerosol observation and sampling instruments, the precious aerosol samples, and the UAV safely from high altitudes using the existing UAV designed for low subsonic flight.

3 The Observation and sample-return system

3.1 The UAV and the Ground Station

The UAV used for the aerosol observation and sample-return flights is shown in Fig.2, and its specifications are shown in Table 1. It has been modified from the UAV used in the same mission at lower altitude in Antarctica (Higashino, et al., 2014, Higashino, et al., 2020) by stretching its nose for a larger payload space, by equipping with flaps for slower flight speed at pull-up maneuverer just after separation, and named as “Phoenix-S”.

Fig.2 Appearance of the Phoenix-S UAV mounted on a preparation stand

https://doi.org/10.5194/amt-2021-234
Preprint. Discussion started: 10 August 2021

Atmospheric Measurement Techniques Discussions

Table 1 Specifications of the Phoenix-S UAV

Item	Value
Wing span	2.9[m]
Total weight	10.5[kg]
Payload weight	2.0[kg]
Wing area	0.58[m^2]
Maximum L/D ratio	14
Maximum airspeed	40[m/s @ sea level]
Power plant	Electric motor
Time for powered flight	5[minutes]

The flight control computer (FCC) system has originally developed by the primary author (Higashino, 2006) using a microcomputer Renesas H8S2638, micro electro mechanical system (MEMS) three-axis accelerometers and rate gyros, a differential pressure sensor, and a GPS receiver The UAV has been modified so that the flaps can be manipulated during the pull-up after dive for slower airspeed. The FCC is thermally insulated by putting it with the batteries in a box made of urethane foam covered by thermal blankets. The thermally insulated FCC hardware has been tested its functions in a thermostatic tank and a low pressure tank by simulating the temperature and pressure profile during the mission up to 30km in altitude. The FCC software has also been developed by the authors (Kawano et al.,2007) using C language, and modified for the two-stage separation. It has seven control modes, and the transition conditions for the entire mission are shown in Table 2. The FCC is

Table 2 Control modes of the FCC software and the conditions for mode transition

Mode name	Transition condition	Function
Launch	Command from GS (ground station)	Maintains trim positions of all control surfaces
Separation	$h \le h_s$	Separates the parachute
Pull-up	$V_a \ge V_s$	Pulls-up the nose of the UAV for the following gliding mode
Glider	$V_a \ge V_c$	Controls airspeed and course for waypoint flight
Normal	Command from the RC transmitter	Controls airspeed, course, and altitude for waypoint flight
Manual	Command from the RC transmitter	Controls the UAV manually
Emergency	Command from GS (ground station) or command from the RC transmitter or $h < h_{\min}$ except in launch mode	Deploys recovery parachute

h : GPS altitude, h_s : second separation altitude, $h_{\min}$: minimum parachute deployment altitude
V_a : airspeed of the UAV, V_s : stalling airspeed of the UAV, V_c : commanded airspeed

https://doi.org/10.5194/amt-2021-234
Preprint. Discussion started: 10 August 2021


Atmospheric Measurement Techniques Discussions

in the launch mode at the beginning of the observation flight until the UAV descend down by the parachute to the second separation altitude. All control surfaces are maintained as pre-set positions in the launch mode. The first separation is performed either by the burst of the balloon or the separator which is connected between the balloon and the descent parachute. After the descent by the parachute, the FCC transitions into the separation mode and separates the parachute when the altitude h becomes smaller than the pre-set separation altitude h_s. The FCC immediately transitions into the pull-up mode, and the airspeed V_a exceeds the stalling speed V_s. It transitions into the gliding mode soon after the airspeed V_a exceeds the commanded gliding speed V_c. The UAV glides back toward the sky over the released point on the ground.

The conventional rate-based gain scheduling PID controller (Kawano et al.,2007) has been implemented in the FCC based on the mathematical model of the UAV obtained by combining the estimated values using DATCOM (DATCOM, 1975), the wind tunnel test results performed at the low-speed wind tunnel at Kyushu University, and the flight test results at lower altitudes.

The ground station was used in order not only to monitor flight trajectory and flight status but also to send commands to the UAV if necessary. The separation of the balloon and the parachute from the UAV is basically performed automatically, and it can also be done manually from the ground station.

3.2 The UAV-balloon system

Fig.3 shows the UAV-balloon just after release, and its components are described in the figure. The UAV was suspended from the balloon, and a parachute (an orange object in the middle of the line seen in Fig.3) was connected between the balloon and the UAV for the descent after first separation. Another small parachute seen just below the balloon in Fig.3 was also connected in order to prevent the descent parachute from collapsing by the fragments of the burst balloon. The third parachute for the final recovery on the ground was stowed in the fuselage of the UAV, and cannot be seen in the figure. The length of the line between the UAV and the parachute was approximately 50m in order to avoid contamination due to the balloon and the parachutes. A shock-absorbing spring and an unwinder which rolls the line off and delays its extension during initial ascent were also connected between the descent parachute and the UAV for easy release. The size of the descent parachute was determined so that the descent speed becomes approximately 7 m/s Equivalent Air Speed (EAS). The rubber balloon called TA3000(TOTEX Co. Ltd.) of which weight is 3000g was used. The parachute separator mounted on the belly of the UAV was composed of a combination of a quick-release snap shackle and a servo motor driven by the FCC. The end loop of the line was hooked up to the snap shackle via a line guide attached to the tail of the UAV in order to avoid the entanglement between the line and the tail control surfaces of the UAV. Another separator using a microprocessor, a pressure sensor, and hot wire could be connected between the balloon and the descent parachute in order for the intended balloon separation at a specific altitude, but it was not used this time.

https://doi.org/10.5194/amt-2021-234
Preprint. Discussion started: 10 August 2021

Atmospheric Measurement Techniques Discussions

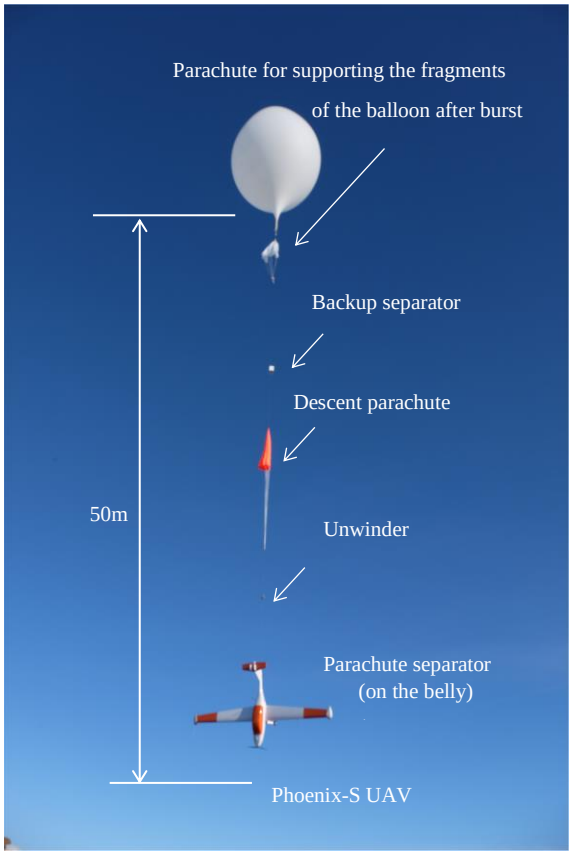

Fig.3 Phoenix-S UAV climbing by a balloon

130

3.3 Aerosol Observation System

An optical particle counter (OPC: ADS-04-UAV, YGK Co. Ltd.) and an airborne aerosol sampler (AAS, Arios Co. Ltd.) were installed in the fuselage of the UAV, and a radio sonde (GPS sonde, RS06G, Meisei Electric Co. Ltd.) was installed in a pod at the right wing tip as shown in Fig.4. The specifications of the OPC is shown in Table 3. The OPC accumulates number of
135 particles by 10 different threshold sizes ranging from 0.3 to 11.4 μm in diameter for every 4 seconds. The specification of the AAS is shown in Table 4. The AAS has been originally developed for the balloon-borne aerosol sampling (Okada et al., 1997) and has been modified for the sampling using a UAV. The AAS is a 2-stage cascade impactor with up to 16 sets of collection media and micro mesh grids. The collection grids are changed automatically in sequential way at every 5 minutes which corresponds to 1.2km in altitude range assuming 4m/s in rate of climb. Two kinds of substrates, a carbon substrate and a nitron
140 substrate were alternately set as shown in Table 5. The carbon substrates were prepared for the analyses of morphology by a SEM (Scanning Electron Microscope) and for the analyses of elements by an EDX (Energy dispersive X-ray analyzer). The

https://doi.org/10.5194/amt-2021-234
Preprint. Discussion started: 10 August 2021

Atmospheric Measurement Techniques Discussions

nitron substrates were specially prepared for the detection of nitrate ions which make crystals by the reaction with nitron, and can be identified by the SEM. Ambient air was introduced to the OPC and the AAS respectively through two separate stainless-steel pipes of which inner diameter is 4.7 mm and the length is 50 mm as shown in Fig.4. The pipes were stood vertically against the side wall of the UAV fuselage. The radio sonde (GPS sonde) transmits temperature, humidity, OPC count, and AAS status data to the ground station by the FM radio waves with its carrier frequency of 403 MHz.

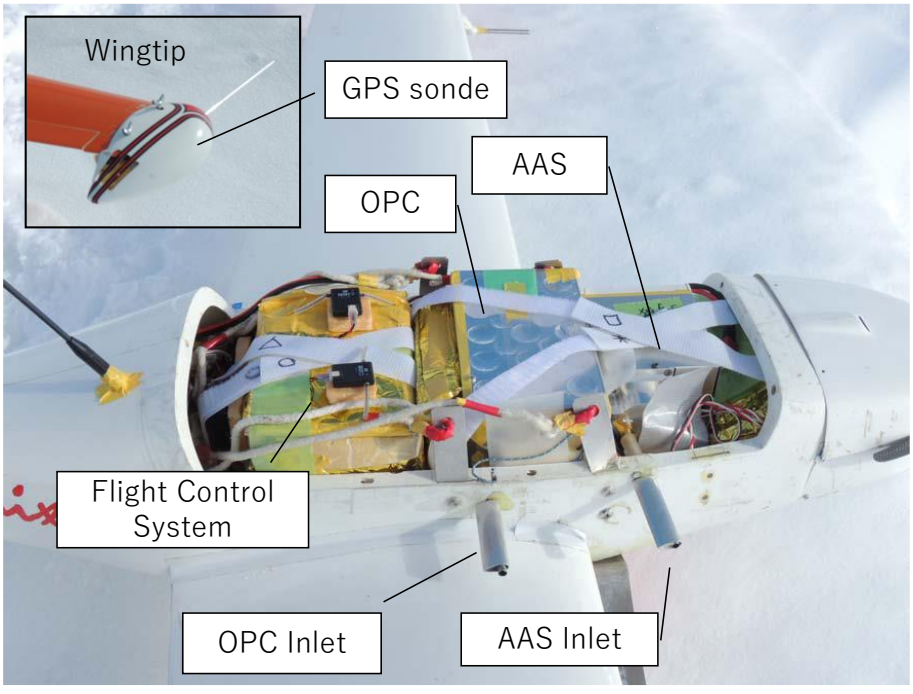

Fig.4 Installation of the optical counter and the onboard aerosol sampler in the fuselage, and the radio sonde(GPS sonde) in the wing-tip pod

Table 3 Specifications of the Optical Particle Counter (OPC)

Light source	Device	Laser diode
	Wave length	780nm, linear polarization
	Output power	50mW
Receiving optics	(side wall scattering)	
	Crossing angle of axis	90 degrees
	Half angle of collection	60 degrees
Measurement	Flow rate	50 cm^3/s
	Integration	4 s
Power	DC	12V, 0.8A
Size	Dimensions	109x92x150mm
	Weight	700g

https://doi.org/10.5194/amt-2021-234
Preprint. Discussion started: 10 August 2021

Atmospheric Measurement Techniques Discussions

Table 4 Specifications of the Airborne Aerosol Sampler (AAS)

Method	2 stage cascade inertial impactor 50% cut-off diameter	1st 1.4 μm , 2nd 0.25 μm at 1atm for sphere with 1g/cm^3
Sampling	Trigger Flow rate Integration Number of samples	Pressure (900hPa, adjustable) or manual 1.6 liter/minute 5 minutes(adjustable, corresponds to 1.2km 16 sets
Data output	2 channels in voltage	Stage rotation motor, sampling pump
Power	DC	12V, 0.7A(max.)
Size	Dimensions Weight	80x105x130mm 650g

Table 5 Sampling altitude ranges and film types for AAS on 24th Jan. 2015

sample No.	sampling altitude(m)			film type
	start	stop	top	
14	22,135	21,337	23,048	nitron
13	20,868	22,135		carbon
12	19,564	20,853		nitron
11	18,349	19,547		carbon
10	17,062	18,326		nitron
9	15,707	17,042		carbon
8	14,163	15,694		nitron
7	12,264	14,148		carbon
6	10,214	12,231		nitron
5	8,149	10,190		carbon
4	6,165	8,116		nitron
3	4,366	6,137		carbon
2	2,698	4,340		nitron
1	1,114	2,675		carbon

4 Prediction of the Flight Trajectory

4.1 Prediction Model

150 In order to perform the observation and sample-return mission successfully, the authors have developed a prediction system of the overall flight trajectory from the climb phase by the balloon, the descent phase by the parachute, and to the gliding phase of the UAV. It considers the climbing speed of the balloon, the drag characteristics of the descent parachute and the UAV, and the lift to drag ratio of the UAV estimated by the wind tunnel tests. The latest prediction of wind speed and direction known

https://doi.org/10.5194/amt-2021-234
Preprint. Discussion started: 10 August 2021


Atmospheric Measurement Techniques Discussions

as Grid Point Value (GPV) data issued by Japan Meteorological Agency are also used. GVP data can be downloaded for free for research and educational purposes at the site of Research Institute for Sustainable Humanosphere, Kyoto University, Japan (GPV data download site).

In the climb phase, position equations of the balloon-UAV system described in the North-East-Down (NED) coordinate system in which its origin is located at the released point of the balloon are shown from eq. (1) to eq.(3). They are numerically integrated until the altitude reaches the assumed first separation altitude.

$$\dot{x} = w_x(x, y, z) \quad (1)$$

$$\dot{y} = w_y(x, y, z) \quad (2)$$

$$\dot{z} = c\,(const) \quad (3)$$

where $w_x(x, y, z)$ and $w_y(x, y, z)$ are wind speed components in x (East) and y (North) direction at the position (x, y, z) respectively. Horizontal wind speed and direction data are taken from the GPV data, and are corrected for the three dimensional position by linear interpolation. No vertical wind speed is considered because no prediction is given in the GPV data. We assumed the climbing speed of the balloon-UAV system as constant from 5 to 7 m/s, and it can be specified arbitrarily.

In the descent phase, the position equations for the horizontal position are the same as eq.(1) and eq.(2), but the vertical position of the parachute-UAV system is shown as eq. (4). The position of the system in descent phase is calculated by numerically integrating eq.(1), eq.(2), and eq.(4) until it reaches the second separation altitude.

$$\dot{z} = \sqrt{2mg / (\rho(z) S C_D)} \quad (4)$$

where m is mass of the parachute-UAV system, g is gravitational acceleration, $\rho(z)$ is air density which is a function of altitude, S is area of the parachute, and C_D is drag coefficient of the parachute-UAV system. We chose the parachute size S and C_D in eq.(4) so that the descent speed becomes approximately 7m/s in equivalent air speed (EAS), but true air speed expressed as eq.(4) changes depending on air density $\rho(z)$ even if the equivalent air speed is assumed as constant (7m/s).

After reaching the second separation altitude, the UAV separates the descent parachute, and the UAV starts gliding back to the released point. The position equations in this gliding phase are shown from eq.(5) to eq.(7).

$$\dot{x} = V\cos(\gamma)\cos(\psi) + w_x(x, y, z) \quad (5)$$

$$\dot{y} = V\cos(\gamma)\sin(\psi) + w_y(x, y, z) \quad (6)$$

$$\dot{z} = V\sin(\gamma) \quad (7)$$

Where V is the true airspeed of the UAV, γ is gliding angle, and ψ is course direction angle of the UAV measured from North. After the separation from the descent parachute, the UAV dives, pulls-up, and turns towards the released point on the ground, but the time for these processes are relatively short, and they are omitted in the prediction for simplicity. In gliding

https://doi.org/10.5194/amt-2021-234
Preprint. Discussion started: 10 August 2021


Atmospheric Measurement Techniques Discussions

180 phase, the UAV glides at the commanded air speed of 28 m/s in EAS, and the true air speed (TAS) changes depending on air density, i.e. flight altitude. The air speed command of 28 m/s was determined considering the best glide speed of the UAV which gives the furthest flight distance determined by the wind tunnel test results, and the mean wind speed based on the examination of the GPV data. The performance of the trajectory prediction will be evaluated in the next section together with the actual flight trajectory.

185

5 Results of observation flights

5.1 Results of trajectory prediction and the observation flights

Three aerosol observation and sample-return flights including one test flight were attempted in Antarctica as shown in Table 6 as one of the 56th JARE (Japanese Antarctica Research Expedition) summer activities in January 2015. Prior to the
190 observation flight, its flight trajectory was predicted using the developed prediction code as mentioned previously. Go/NoGo decision was made considering multiple information sources not only the result of the flight trajectory prediction, but also the weather forecasts of Antarctic Mesoscale Prediction System (UCAR, 2021), "Balloon Trajectory Forecasts" of Wyoming University (UWYO, 2021), and in-situ weather observation on the ground.

Table 6 Results of the observation and sample-return flights in Jan. 2015

Flight No.	No.1	No.2	No.3
Max. altitude (km) for aerosol concentration observation	6	23	16
Cause of max. altitude	Intentional	Burst	Burst
Max. altitude (km) for aerosol sampling	6	22	N.A.
Aerosol sample returned	Yes	Yes	No

Fig.5 shows the flight trajectory of flight No.2 in which the maximum altitude reached 23km, and aerosol sample at 22km was
195 returned. The first separation was planned at 30km in altitude, but the rubber balloon burst at 23km. The UAV started descent by the parachute until 12km, and then started gliding by separating the parachute. After the UAV arrived over the released point, it continued gliding over the released point along a rectangular pattern as shown in Fig.5. Finally, the UAV was recovered by another parachute on the ice floor as shown in Fig.6. All these processes are carried out autonomously except for the final recovery by the parachute.

200

https://doi.org/10.5194/amt-2021-234
Preprint. Discussion started: 10 August 2021

Atmospheric Measurement Techniques Discussions

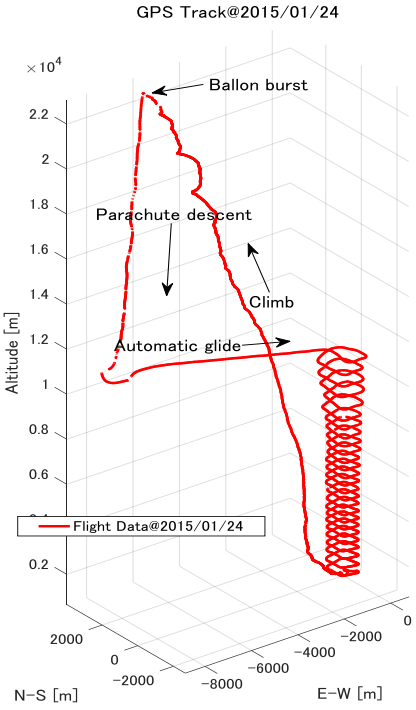

Fig.5 Trajectory of flight No.2 on 24th Jan. 2015

Fig.6 Final recovery of the UAV by a parachute

Fig.7 compares the actual trajectory in flight No.2 in a horizontal plane in red solid line with the four predicted trajectories for two different times using GPV data issued at two different times. The observation flight was planned around 15:00UTC on

https://doi.org/10.5194/amt-2021-234
Preprint. Discussion started: 10 August 2021

Atmospheric Measurement Techniques Discussions

24th January 2015, but the GPV forecast data only for 12:00UTC and 18:00UTC are available. For this reason, the flight trajectory starts at12:00 UTC and 18:00 UTC were predicted using the GPV data issued at one day and two days before the
205 flight. The trend of the change in flight trajectory predictions how the balloon-UAV system would drift looks rotating to the left as indicated as red arrows in the figure, and they look getting closer to that in actual trajectory. Although the difference between the horizontal positions of the separation points in actual flight and the last prediction were approximately 6 km, the prediction can be said to be relatively reliable.

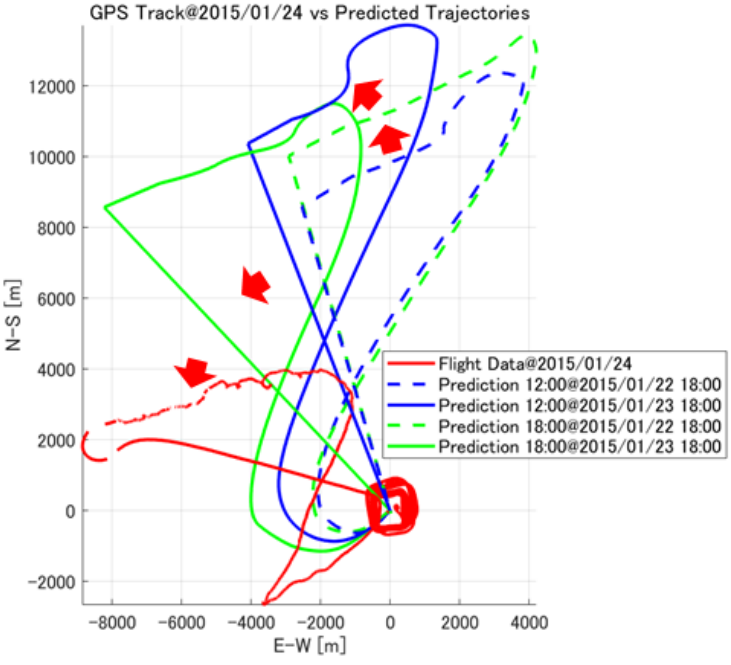

Fig.7 Actual trajectory of flight No.2 on 24th Jan. 2015 in the horizontal plane and the predicted trajectories at different forecasted time

https://doi.org/10.5194/amt-2021-234
Preprint. Discussion started: 10 August 2021

Atmospheric Measurement Techniques Discussions

5.2 Preliminary results of the aerosol observation and sampling

5.2.1 Concentration of aerosols observed by the OPC

The vertical profiles of aerosol concentrations in accumulation mode are shown in Fig.8. Stratospheric aerosol layer is seen between 9.5 km (tropopause) and 23 km in altitude, and it is composed of three sublayers with maximum concentrations of 2, 2.5, and 3.7 particles/cm3 for d > 0.3 μm at around 16, 12, and 10 km in altitude respectively. These concentrations looks different from the typical concentration profile in Antarctic summer stratospheric aerosol layer of which maximum concentration is approximately 1.0 particles/cm3 without sublayers (Kizu et al., 2010). One of the possibilities for explaining the difference is the injection of volcanic ash. Mt. Kelut (7° 55' 48" S, 112° 18' 29" E, 1731m) erupted at 22:50 LT on February 13, 2014 (NASA 2021), and it is reported that ash clouds were found around 20 km and its plume seemed to reach around 30 km in altitude. Although further investigation is necessary, there is a possibility of volcanic injections in stratosphere which spread globally and reached Antarctic stratosphere.

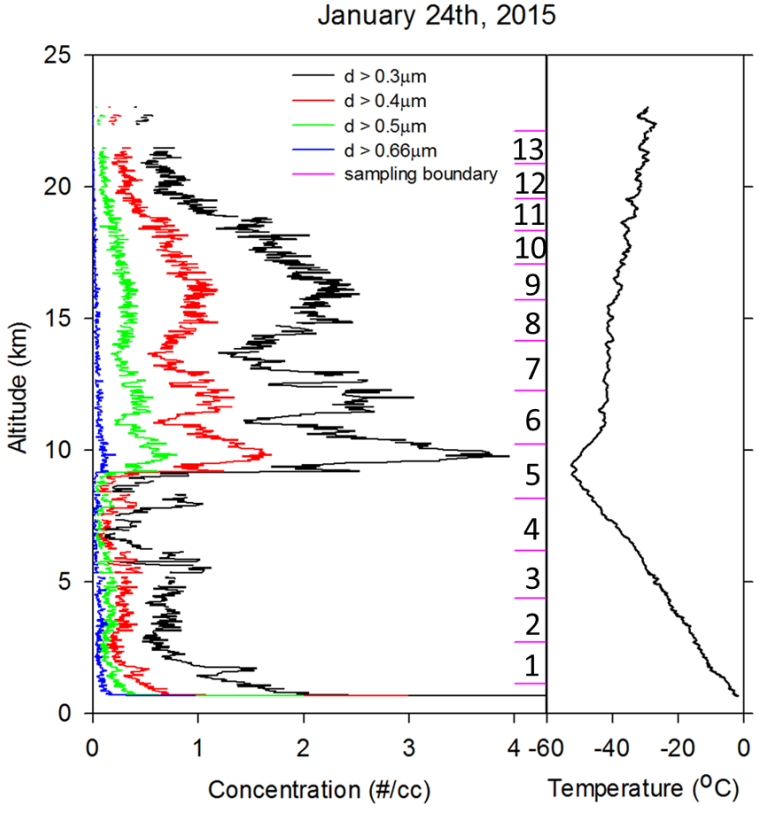

Fig.8 Vertical profile observed by UAV borne OPC on January 24, 2015

left: aerosol concentration, right temperature, numbers show sample ID shown in Table 5

https://doi.org/10.5194/amt-2021-234
Preprint. Discussion started: 10 August 2021

Atmospheric Measurement Techniques Discussions

5.2.2 Constituent analyses by SEM/EDX

Sampling altitude ranges and film types on the observation flight No.2 on 24th Jan. 2015 are summarized in Table 7. The inclusion of sulfuric acid and mineral examined by morphology, and the characteristics observed by X-ray analyses are summarized in the column of "sulfate" and "mineral" in Table 7. The particles including Si and Al are classified as "mineral", and S (sulfur) as "sulfate". Two examples of a SEM image of particles on nitron regent thin film are shown in Fig.9 and Fig.10. The particles in Fig.9 were collected at 14.2～15.7 km in altitude, and the particles in Fig.10 were collected at 10.2～12.2 km. All particles in Fig.9 are crystal-like ones, and it implies that the inclusion of nitrate ion occurred. However, it is against our expectations that the nitric acid can be formed because the air temperature at the altitude was relatively high (around -45 degrees Celcius) for the inclusion of nitrate ion. A similar morphology was found from the cold stratosphere in Arctic winter (Iwasaka et al., 1993) in which the air temperature was lower than -80 degrees Celcius, but the sizes of the crystals in Fig.9 looks smaller than 1 μm, and they are smaller than those found from the cold stratosphere in Arctic winter. They indicate unusual inclusion of nitrate ion in stratospheric aerosols under "warm" summer conditions. It is difficult to understand how they are produced in view of common knowledge. There are several possibilities for explaining the cause of the result such as quaternary aerosol of HCl/HNO3/H2SO4/H2O caused by high HCl concentration by volcanic injection, high HNO3 concentration caused by oxidation of N2 with high energy reaction by thunder, residue of HNO3 in stratospheric aerosols by hysteresis of production of ternary aerosols of HNO3/H2SO4/H2O in winter. However further investigation is necessary to understand how they are produced.

Table 7 Type of individual aerosol by SEM/EDX analyses (24th Jan. 2015)

sample No.	sampling altitude(m)		film type	sulfate	nitrate	mineral
	start	stop				
10	17,062	18,326	nitron	major	non	non
9	15,707	17,042	carbon	major	-	non
8	14,163	15,694	nitron	-	major	non
7	12,264	14,148	carbon	major	-	non
6	10,214	12,231	nitron	major	minor	non
5	8,149	10,190	carbon	major	-	rare
4	6,165	8,116	nitron	major	minor	rare
3	4,366	6,137	carbon	major	-	rare
2	2,698	4,340	nitron	-	minor	rare

Two types of particles are seen in Fig.10 judging from their appearances. One is spherical, and it looks like a liquid droplet. The same type particles occupies most of the particles. The other looks like a crystal. The analysis showed that the crystal-like

https://doi.org/10.5194/amt-2021-234
Preprint. Discussion started: 10 August 2021

Atmospheric Measurement Techniques Discussions

particles are nitric acid particles, while the droplet-like particles did not include nitric acid. It implies that they are composed of sulfuric acid. Similar crystals were not found between 17.1 and 18.3 km in altitude.

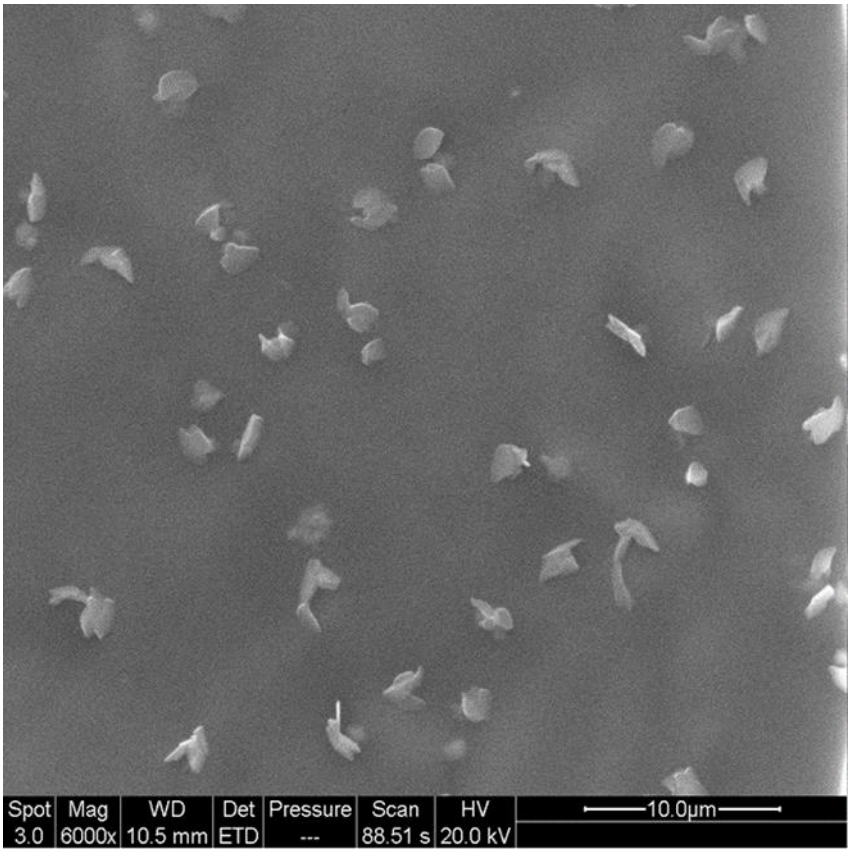

Fig.9 Morphology of aerosols sampled on nitron thin film collected at 14.2～15.7 km, on January 24, 2015

6 Conclusion

245 The authors have proposed the "two-stage separation method" for the stratospheric aerosol observation and sample-return using the combination of a rubber balloon, a descent parachute, and a gliding UAV. In this method, observation instruments are installed in the UAV, and the UAV suspended by the balloon climbs up to stratospheric altitudes while aerosol observation and sampling are conducted. After reaching the target altitude or the burst of the balloon, the UAV descends down by the descent parachute to a certain altitude at which the flight control system of the UAV works properly. The UAV is then separated

https://doi.org/10.5194/amt-2021-234
Preprint. Discussion started: 10 August 2021

Atmospheric Measurement Techniques Discussions

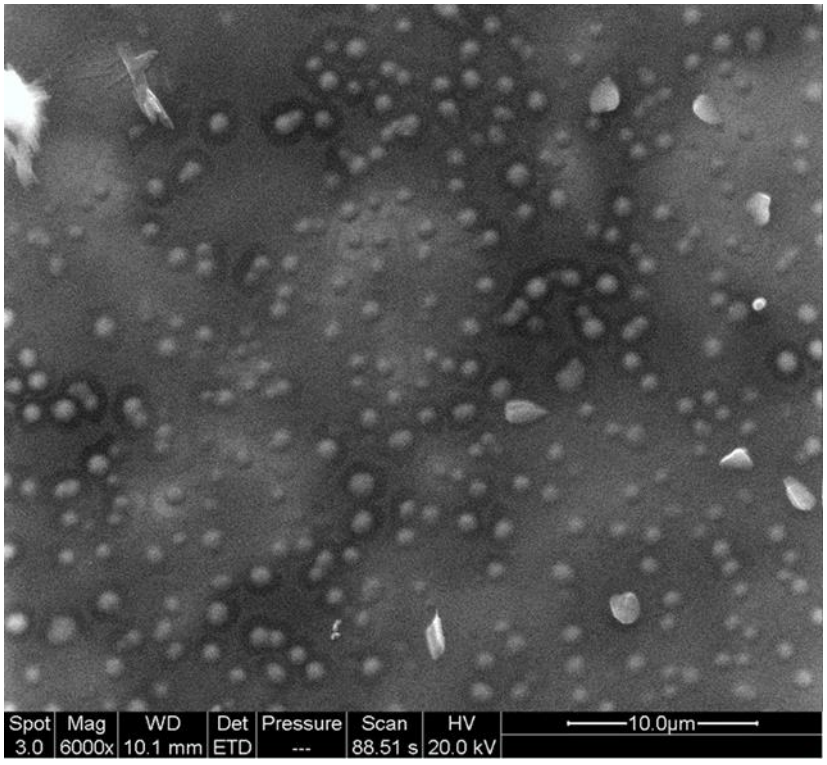

Fig.10 Morphology of aerosols sampled on nitron thin film collected at 10.2～12.2 km, on January 24, 2015

from the descent parachute, and it starts gliding back to the released point on the ground autonomously. This method was attempted and proved to be quite effective in Antarctica in one of the JARE56 summer activities. The aerosol observation up to the altitude of 23km and aerosol sampling up to 22km were achieved. The UAV started gliding from 12km in altitude and the UAV as well as the samples and the observation instruments are successfully recovered.

A trajectory prediction system using the aerodynamic characteristics of the UAV and GPV data was developed. It was used for the Go/NoGo decision of the operation, and the comparison of the predicted flight trajectories and the actual flight trajectory showed relatively good agreement.

The obtained vertical aerosol concentration profile showed three sub-layers in the stratosphere, and the concentrations of them were unusually high compared to a typical concentration level of the stratospheric aerosol layer in Antarctic summer which does not have sub-layers. Although further investigation is necessary, there is a possibility of volcanic injections in stratosphere due to the eruption of Mt.Kelut on February 13, 2014. By constituent analyses of the returned sample, a number of nitric acid particles were found in the stratosphere in spite of the relatively high temperature around -45 degrees Celsius for the inclusion of nitrate ion. Although all the results regarding the aerosol concentration profile and constituent analyses by SEM require further investigation, the results showed that the system using the balloon-assisted UAV using two-stage-separation method is

https://doi.org/10.5194/amt-2021-234
Preprint. Discussion started: 10 August 2021


Atmospheric Measurement Techniques Discussions

quite useful, and it has a capability to produce more opportunities to observe and collect aerosol samples which may lead to new knowledge.

References

BAS (2008): Unmanned aerial vehicles mark robotic first for British Antarctic Survey, Press release, Issue date: 18 Mar. 2008, Number: 09/2008 (online), https://www.bas.ac.uk/media-post/unmanned-aerial-vehicles-mark-robotic-first-for-british-antarctic-survey/ (accessed 2021-4-10)

DATCOM : USAF Stability and Control DATCOM, Flight Control Division, Air Force Flight Dynamics Laboratory, Wright-Patterson Air Force Base, Ohio, Jan. 1975.

Funaki, M., Higashino, S., Sakanaka, S., Iwata, N., Nakamura, N., Hirasawa, N., Obara, N., Kuwabara, M. (2014): Small unmanned aerial vehicles for aeromagnetic surveys and their flights in the South Shetland Islands, Antarctica. Polar Science 8 (2014) 342-356, 2014.

GPV data download site: http://database.rish.kyoto-u.ac.jp/arch/jmadata/data/gpv/original/ (accessed 2021-6-10)

Hara, K., Iwasaka, Y., Wada, M., Ihara, T., Shibata, H., Osada, K., and Yamanouchi, T. (2006) : Aerosol constituents and their spatial distribution in the free troposphere of coastal Antarctic regions, J. Geophys. Res., 111, D15216, doi:10.1029/2005JD006591.

Hara, K., K. Osada and T. Yamanouchi (2013): Tethered balloon-borne aerosol measurements: Seasonal and vertical variations of aerosol constituents over Syowa Station, Antarctica. Atmos. Chem. Phys. 13, 9119-9139, doi:10.5194/acp-13-9119-2013.

Hara, K., M. Hayashi, M. Yabuki, M. Shiobara and C. Nishita-Hara, (2014): Simultaneous aerosol measurements of unusual aerosol enhancement in troposphere over Syowa Station, Antarctica. Atmos. Chem. Phys., 14, 4169-4183, doi:10.5194/acp-14-4169- 2014.

Hayashi, M., Y. Iwasaka, M. Watanabe, T. Shibata, M. Fujiwara, H. Adachi, T. Sakai, M. Nagatani, H. Gernandt, R. Neuber, M. Tsuchiya. (1998) : Size and Number Concentration of Liquid PSCs -Balloon-Borne Measurements at Ny-Ålesund, Norway in Winter of 1994/95-, J. Meteorol. Soc. Japan, 76, 549-560, DOI: https://doi.org/10.2151/jmsj1965.76.4_549, 1998.

Higashino, S. (2006): Development of an UAV Flight Control Module for the Operation in Antarctica, The 5th Asian-Pacific Conference on Aerospace Technology and Science, CD-ROM, 2006.

Higashino, S., Funaki, M. (2013) : Development and Flights of Ant-Plane UAVs for Aerial Filming and Geomagnetic Survey in Antarctica. J. Unmanned Sys Tech, 1, 37-42, 2013.

https://doi.org/10.5194/amt-2021-234
Preprint. Discussion started: 10 August 2021


Atmospheric Measurement Techniques Discussions

Higashino, S., Hayashi, M., Nagasaki, S., Umemoto, S., Nishimura, M. (2014) : A Balloon-Assisted Gliding UAV for Aerosol Observation in Antarctica, Trans. JSASS Aerospace Technology Japan, 12, APISAT-2013, a35-a41, 2014.

Higashino, S., Hayashi, M., Umemoto, S., Nagasaki, S., Nishimura, M., Ozuka, K., Shiraishi, K., and Naganuma, A.(2020) : Development of Balloon-Assisted Gliding Unmanned Aerial Vehicle System for Atmospheric Observation and Spatiotemporal Aerosol Variations in Summer Troposphere over Syowa Station, Nankyoku Shiryo(Antarctic Record), Vol.65. pp.21-44, 2020. (In Japanese with English abstract)

Ito, T., Morita, Y. and Iwasaka, Y. (1986) : Balloon Observation of Aerosols in the Antarctic Troposphere and Stratosphere, Tellus B : Chemical and Physical Meteorology, 38, 214-222.

Iwasaka, Y., Okada, K. and Ono, A. (1985) : Individual aerosol particles in the antarctic upper troposphere, Mem. Natl. Polar Res, Special Issue 39, 17-29.

Iwasaka, Y., M. Hayashi, Y. Kondo, M. Koike, S. Koga, M. Yamato, P. Aimedieu, W. A. Matthews (1993): Two Different Type Nitrate Aerosols in the Winter Polar Stratosphere: Morphology of Individual Particles Observed with an Electron Microscope, J. Geomag. Geoelect., 45, 1181-1192, DOI https://doi.org/10.5636/jgg.45.1181, 1993

Kawano, M., Kozai, S, and Higashino, S. : Development of an Autonomous UAV Using a simple avionics and its Flight Tests, 45th Aircraft Symposium , Japan Society for Aeronautics and Astronautics, CD-ROM (In Japanese with English abstract), 2007.

Kizu, N., M. Hayashi, T. Yamanouchi, Y. Iwasaka, M. Watanabe (2010): Seasonal and annual variations of aerosol concentrations in the troposphere and stratosphere over Syowa Station observed by a balloon-borne optical particle counter, Mankyoku Siryo (Antarctic Record), 54, 760-778, (in Japanese with English abstract), 2010.

NASA(2021) : Indonesia's Mount Kelut Erupts:NASA earth observatory, https://earthobservatory.nasa.gov/images/83144/indonesias-mount-kelut-erupts (accessed 2021-6-3)

Okada, K., Wu, P.M., Tanaka, T., and Hotta, M. (1997) : A Light Balloon-Borne Sampler Collecting Stratospheric Aerosol Particles for Electron Microscopy, J. Meteorol. Soc. Japan, 76, 549-560, DOI https://doi.org/10.2151/jmsj1965.75.3_753, 1997.

Spiess, T., Bange, J., Buschmann, M. and Vörsmann, P. (2007): First application of the meteorological Mini-UAV 'M2AV' . Meteorol. Z., 16, 159–169, doi: 10.1127/0941–2948/2007/0195.

Stocker, T.F., D. Qin, G.-K. Plattner, M. Tignor, S.K. Allen, J. Boschung, A. Nauels, Y. Xia, V. Bex and P.M. Midgley (2013) : IPCC, 2013: Climate Change 2013: The Physical Science Basis. Contribution of Working Group I to the Fifth Assessment Report of the Intergovernmental Panel on Climate Change, Cambridge, United Kingdom and New York, NY, Cambridge University Press, 1535 p.

UCAR (2021): The Antarctic Mesoscale Prediction System: University corporation for atmospheric research. Updated every day. https://www2.mmm.ucar.edu/rt/amps/ (accessed 2021-6-3). (accessed 2021-6-3)

UWYO (2021): Upper Air Data, Balloon Trajectory Forecasts: University of Wyoming. Updated every day. http://weather.uwyo.edu/upperair/balloon_traj.html (accessed 2021-6-3).

https://doi.org/10.5194/amt-2021-234
Preprint. Discussion started: 10 August 2021


Atmospheric Measurement Techniques Discussions

Yamanouchi, T., Wada, M., Fukatsu, T., Hayashi, M., Osada, K., Nagatani, M., Nakada A., and Iwasaka, Y.(1999): Airborne observation of water vapor and aerosols along Mizuho route, Antarctica, Polar Meteorol. Glaciol., 13, 22–37.

Yamanouchi, T. (2010) : Progress of "Study on Polar Atmospheric Circulation and Material Cycle", Antarctic Record, 54, 245-273 (In Japanese with English abstract).

Author contribution

S.Higashino and M.Hayashi designed the experiment. S.Higashino, T.Okada, and S.Nagasaki developed the UAV system, and M.Hayashi and K.Ozuka developed the OPC and AAS. S.Higashino and T.Okada carried out the experiment in Antarctica. M.Hayashi and K.Shiraishi performed the analyses of the aerosol concentration and constituent of the samples. S.Higashino prepared the manuscript with contributions from all co-authors.

Acknowledgement

The authors would like to thank to all expedition members of the 56th Japanese Antarctic Research Expedition (JARE), the wintering member of the 55th JARE, and the captain and the crew of icebreaker ship Shirase for observation flights at Syowa Station. The avionics and UAV are made by the cooperation of Mr. Manabu Matsubara, Mr. Tadashi Nagayasu, Mr.Hiroshi Kinjyo of Kyushu University, and Mr. Rattanarrom of X-Treme Composite Thailand. Domestic flights tests are conducted by the cooperation of the students of Flight dynamic Lab. of Kyushu University and Atmospheric Material Science Lab. of Fukuoka University, Mr. Ino of Aso Kanko ranch, Mr.Yagyu of Matsuyama farm, the Japan Civil Aviation Bureau. The flight tests in Mongolia is conducted by the cooperation of Professor Obikane and other staffs and students of Mongolian University of Science and Technology. This work was supported by AP11, AP41 of National Institute of Polar Research and JSPS Kakenhi grant number 23651019 and 24403001.